THE IDRIFF TWO-PHASE SIMULATION CODE AND ITS APPLICATION TO THE STUDY OF A PRESSURIZER

Multi-Phase Transport & Particulate Phenomena, Hemisphere Pres, New York.
also 4th Miami Int. Symp. on MPT & PP, Dec 96, Miami

R. Sollychin, W.J. Garland and J.S. Chang
Department of Engineering Physics
McMaster University
Hamilton, Ontario
L8S 4M1

ABSTRACT

The IDRIFF simulation code has been developed as a convenient tool in the analyses of two-phase flow which occasionally requires detailed information on local phenomena in the flow. The code consists of two major model components: (1) lumped formulation for the fluid conservation equations and the equation of state; (2) sets of one-dimensional drift-flux equation and the equation of state written in differential forms.

A small scale pressurizer made of a glass tank and its associated systems were set up to simulate the behaviour of a nuclear power plant pressurizer. A version of the IDRIFF code is specially designed to simulate the experiments such that any particular pressurizer phenomena (or parameter) of interest can be calculated in detail without the necessity of performing unnecessary detailed calculations on other aspects as well.

The result of the simulation is in good agreement with experimental measurements. Interpolation and extrapolation of experimental data by the IDRIFF code simulation has initially resulted in: (1) relationships between the void fraction in the pressurizer and pressurizer boundary condition; and (2) a flow-regime map of pressurizer under quasi-steady-state conditions.

1. INTRODUCTION

The main objective of developing the IDRIFF (Integrated Drift-Flux Formulation) code is to provide a flexible tool in the analysis of two-phase flow which occasionally requires detailed information on local phenomena in the flow. The IDRIFF code has two major model components: one with governing equations written in lumped forms, and the other with sets of differential forms of governing equations. In addition, various physical submodels and code control features are incorporated into the code.

Many pressurizer models are reported in the literature or currently used in the nuclear industry. Examples are those developed by Gorman [1], Nahavandi and Makkenchery [2], and Baggoura and Martin [3]. In most of them, the thermodynamic state(s) of the fluid in the pressurizer is pre-assumed. Mathematical models are then set up based on this assumption. The models are usually adequate in predicting pressurizer behaviour qualitatively. However, inconsistent performance of the models for different power plant transients is generally reported [4,5]. It is believed that the major drawback of these pressurizer models is due to the lack of understanding on the detailed physical phenomena in the pressurizer. There has been a renewed interest in the systematic study of local thermalhydraulic phenomena in the pressurizer. An example is the work by Griffith and his coworkers [5], in which phenomena such as heat transfer to wall, interface mass transfer and stratification of insurge fluid have been investigated. Simulation of the behaviour of a pressurizer using a sophisticated system code has also been attempted [6]. In the present study of the pressurizer, problems such as the effect of boundary conditions, pressure, temperature and void fraction profiles, and quasi-steady-state flow-patterns are

investigated as well. A highly flexible simulation tool is therefore needed such that any physical phenomena in the pressurizer can be simulated and that if a particular phenomena (or a parameter) is to be investigated, detailed information about the phenomena (or parameter) can be obtained without the necessity of performimg unnecessary detailed calculations on other aspects as well. A version of the IDRIFF code is specially designed to meet this requirement and will be discussed in this paper.

A general description of the IDRIFF code is presented in the following section. The mathematical models of the code will be summarized in section 3. The method of applying the code in the study of the pressurizer will be discussed in section 4. Finally, one particular aspect of the application: the generation and analysis of pressurizer quasi-steady-state data will be presented in section 5.

2. GENERAL DESCRIPTION OF THE IDRIFF CODE

The basic structure of the IDRIFF code is a set of fluid mass, energy, and volume balance equations and the equation of state, written in lumped (integrated) form. The pressurizer is divided into two control volumes, with the one dominated by the gas phase geometrically above the liquid phase dominated one. The lumped formulation is then applied to each of the control volumes. The size of both control volumes are dynamically adjusted according to the calculation of swelling or shrinking in the lower control volume, which is dominated by the liquid phase.

The IDRIFF code provides a unique and powerful feature: when there is a need to obtain detailed profiles of flow parameters in any one or more of the control volumes, the lumped formulation on the control volume(s) can be replaced by sets of one-dimensional drift-flux model formulations. The drift-flux formulation consists of five differential equations: mixture continuity, mixture momentum, mixture energy, dispersed phase continuity and equation of state.

From experimental observation, it is found that the possible flow-regimes in the bottom control volume are single-phase liquid, bubbly flow, froth flow and bubbly/froth mixture. The flow-regime in the top control volume is either single-phase vapour or droplet flow. For both volumes, therefore, only one type of drift-flux formulation is required, that is, one suitable for dispersed flow. For numerical convenience, however, two sets of this type of drift-flux formulation are prepared, one for the flow-regime in which the liquid phase is the continuum phase and one for the flow-regime in which the gas phase is the continuum phase.

The IDRIFF code is an interactive, highly flexible computer code currently residing at McMaster University on a VAX 8600. Before and during a simulation, each control volume is divided into grid-points to which the drift-flux formulation is applied when required. The number of grid-points is dynamically determined by the size of the control volume and by the size of the increment between grid-points. The latter is pre-set by the user for an individual control volume. When the drift-flux formulation is used in the calculation of a control volume, the program time-step is divided into sub-time-steps, the number of which is user controlled and is applicable only to that particular control volume. At the end of each time-step, upon a signal from the keyboard, access to the program run-control is available to the user, so that choices on the type of model (lumped or drift-flux, local mechanical equilibrium or non-equilibrium), divisions of time-step into sub-time-steps, and type of output (screen display, storing into files, hard-copy or any combinations of the above) can be made by the user.

When the drift-flux formulation is used, values of local drift-flux parameters are integrated over the control volume and their volume-averaged values are determined. The purpose of obtaining these averaged values is two-fold. First, averaging ensures that the drift-flux formulation is compatible with the rest of the IDRIFF models' structure, which is based on the lumped formulation. Second, the averaged values are used to setup boundary conditions for neighboring control volumes. The swell and shrink of the control volume are calculated based on the results of the lumped model (mass inventory and movement of interface due to pressure difference between the liquid control volume and the steam control volume) and the integrated results of the drift-flux model (void fraction). The approach of using the drift-flux concept to calculate liquid level in a lumped pressure vessel model is similar to that by Wulff et al. [7], except that, in the latter, the expression estimating the liquid level is analytically

derived from the drift-flux concept. In the present work, however, the drift-flux differential equations are solved locally at each grid-point and the results are numerically integrated. Based on the new volume, the grid-points are reorganized at each time step and the values of the drift-flux parameters over the new grid-points structure in the control volume are distributed.

3. MATHEMATICAL MODELS

The basic modelling principle adopted in the IDRIFF code facilitates the simulation of mechanical and thermal non-equilibrium in the pressurizer. In the lumped formulation, there is a non-equilibrium between the two control volumes. In the drift-flux formulation, local thermal (and mechanical as well, if desired) non-equilibrium between the two phases is modelled at each grid-point. A detailed description of the models has been presented by Sollychin et al. [8] and is summarized in this section.

Lumped Formulation

Figure 1 shows the schematic of the control volumes. The individual rate of change of mass in the control volumes can be expressed as follows :

$$\frac{dM_S}{dt} = -W_{STB} - W_{CD} - W_{CI} + W_{EI} + W_{BR} \tag{1}$$

$$\frac{dM_L}{dt} = W_{SRL} - W_{EI} - W_{BR} + W_{CD} + W_{CI}, \tag{2}$$

where W_{STB} is the steam bleed flow, W_{SRL} is the surge-line flow, W_{CI}, W_{EI}, W_{BR} and W_{CD} are various terms representing mass exchanges between the two control volumes.

Similarly, the rate of change of energy in the two control volumes can be expressed by as follows:

$$\frac{dH_S}{dt} = -(W_{STB} \cdot h_{gST}) - (W_{CD} \cdot h_{fST}) - (W_{CI} \cdot h_{gST}) + (W_{EI} \cdot h_{gLQ})$$

$$+ (W_{BR} \cdot h_{gLQ}) - Q_{WS} + Q_{TR} - (1-\beta)[(1-\delta)\, Q_{COND} + Q_{EVPR}] \tag{3}$$

and

$$\frac{dH_L}{dt} = -(W_{SRL} \cdot h_{SRL}) - (W_{EI} \cdot h_{fLQ}) - (W_{BR} \cdot h_{gLQ}) + (W_{CI} \cdot h_{fST})$$

$$+ (W_{CD} \cdot h_{fST}) - Q_{WL} + Q_{HEATR} - Q_{TR} - \beta\,[(1-\delta)Q_{COND} + Q_{EVPR}], \tag{4}$$

In addition to the energy flux terms associated with mass flux, various heat source and sink terms are included: Q_{HEATR} is the heat input to the fluid from the heaters; Q_{WS} and Q_{WL} are the rate of heat loss to the wall in the steam control volume and in the liquid control volume, respectively; Q_{TR} is the heat transfer rate from the liquid control volume to the steam control volume due to any temperature gradient, excluding those due to interface evaporation and condensation; Q_{COND} is the rate of energy released by the condensing steam at the interface; and Q_{EVPR} is rate of energy absorbed by the evaporating liquid at the interface.

It is assumed that the liquid (bottom) control volume, which is dominated by liquid phase, is much more incompressible than the steam (top) control volume, which is dominated by the gas phase. Hence the calculation of swell and shrink is only done for the liquid control volume. In addition, constant total volume gives:

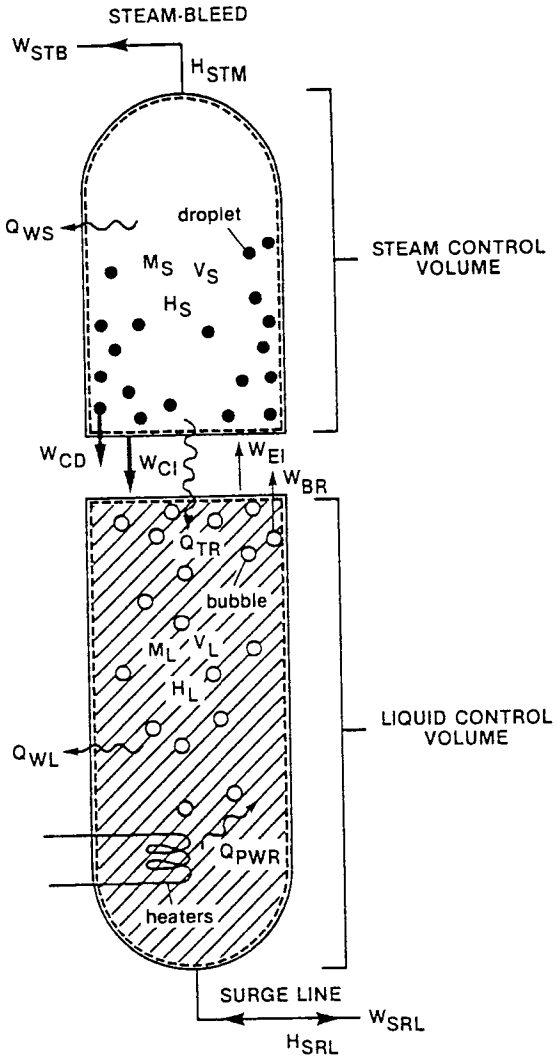

FIGURE 1. Schematic of pressurizer control volumes.

$$\frac{dV_S}{dt} = -\frac{dV_L}{dt} . \tag{5}$$

In addition, a simplified momentum equation is implemented. Due to the nature of the pressurizer , where the liquid is basically stagnant, the momentum equation is used to calculate only the vertical movement of the liquid surface due to pressure difference between the steam control volume and the liquid control volume, as mentioned previously.

Furthermore, the following are implemented as parts of the lumped formulation component of the code: bubble rise submodel, droplet drop submodel, interface evaporation and condensation submodel, steam-bleed flow submodel, surge-line flow submodel, heat generation from electrical heaters and calculations of heat distribution due to heat evaporation and condensation (parameters β and δ).

The steam control volume and the liquid control volume are assumed to be at each of their own saturation condition under their respective average pressures. Hence, the thermodynamic properties of the steam control volume and the liquid control volume are functions of their respective average pressures and qualities.

Drift-Flux Formulation

The basic concept of the drift-flux model is that the dynamics of the two-phase mixture as a whole can be expressed by a mixture momentum equation, and the relative motion between phases by a kinematic constitutive equation, namely the calculation of the drift-velocity v_{dj} defined as:

$$v_{dj} = (1 - \langle \alpha_d \rangle)(\langle\langle v_d \rangle\rangle - \langle\langle v_c \rangle\rangle) \tag{6}$$

The time averaged three-dimensional form of the drift-flux model's equations have been derived by Ishii [9]. Using area averaging, the equations can be converted into the following one-dimensional forms, and used as the governing equations in the drift-flux component of the IDRIFF code:

Mixture continuity equation:

$$\frac{\partial \langle \rho_m \rangle}{\partial t} + \frac{\partial}{\partial z}(\langle \rho_m \rangle \bar{v}_m) = 0 ; \tag{7}$$

Continuity equation for the dispersed phase:

$$\frac{\partial \langle \alpha_d \rangle \rho_d}{\partial t} + \frac{\partial}{\partial z}(\langle \alpha_d \rangle \rho_d \bar{v}_m) = \langle \Gamma_d \rangle - \frac{\partial}{\partial z}\left(\frac{\langle \alpha_d \rangle \rho_d \rho_c}{\langle \rho_m \rangle} v_{dj} \right); \tag{8}$$

Mixture momentum equation:

$$\frac{\partial \langle \rho_m \rangle \bar{v}_m}{\partial t} + \frac{\partial}{\partial z}(\langle \rho_m \rangle \bar{v}_m^2) = \frac{\partial}{\partial z}\langle P_m \rangle + \frac{\partial}{\partial z}\langle \tau_{zz} + \tau_{zz}^T \rangle$$

$$- \langle \rho_m \rangle g_z - \frac{f_m}{2D}\langle \rho_m \rangle \bar{v}_m |\bar{v}_m| - \frac{\partial}{\partial z}\left[\frac{\langle \alpha_d \rangle \rho_d \rho_c}{(1 - \langle \alpha_d \rangle)\langle \rho_m \rangle} v_{dj}^2 \right]$$

$$- \frac{\partial}{\partial z} \sum_k \mathrm{COV}(\alpha_k \rho_k v_k v_k) + \langle M_m \rangle ; \tag{9}$$

Mixture enthalpy energy equation :

$$\frac{\partial \langle \rho_m \rangle \bar{h}_m}{\partial t} + \frac{\partial}{\partial z}(\langle \rho_m \rangle \bar{h}_m \bar{v}_m) = -\frac{\partial}{\partial z}\langle q + q^T \rangle + \frac{q_w'' \xi_h}{A}$$

$$- \frac{\partial}{\partial z}\left[\frac{\langle \alpha_d \rangle \rho_d \rho_c}{\langle \rho_m \rangle} \Delta h_{dc} v_{dj} \right] - \frac{\partial}{\partial z} \sum_k \mathrm{COV}(\alpha_k \rho_k h_k v_k) +$$

$$+ \frac{\partial}{\partial z}\langle P_m \rangle + \left[\bar{v}_m + \frac{\langle \alpha_d \rangle \rho_d \rho_c}{\langle \rho_m \rangle} v_{dj} \right] \frac{\partial \langle P_m \rangle}{\partial z} + \langle \Phi_m^\mu \rangle + \langle \Phi_m^\sigma \rangle + \langle \Phi_m^i \rangle . \tag{10}$$

The local area-averaged mixture pressure $\langle P_m \rangle$, which is defined as:

$$\langle P_m \rangle = \langle \alpha_d \rangle P_d + (1 - \langle \alpha_d \rangle) P_c \tag{11}$$

is assumed to be the saturation pressure of the mixture at the local grid point. When local mechanical equilibrium is assumed, the value of phase pressure, P_d and P_c, are set equal to $\langle P_m \rangle$. Otherwise, if

local mechanical non-equilibrium calculation is desired, the values of P_d and P_c at each grid-point are determined, in addition to Eqn. (11), by the following:

$$P_d = P_c + \Delta P \tag{12}$$

where ΔP is the local interphase pressure difference due to outer surface tension of the dispersed particles such as bubbles and droplets.

From a thermal non-equilibrium point of view, the dispersed phase is assumed to be at saturation locally with respect to the local dispersed phase pressure. On the other hand, the continuum phase is allowed to depart from its saturation state locally with respect to the local continuum phase pressure. The local continuum phase temperature is determined by the local continuum phase pressure as well as the local continuum phase specific enthalpy.

Equation of State

The pressurizer is operated at pressures ranging from 60 kpa(a) to 300 kpa(a), where water thermo-dynamic properties vary drastically with pressure. Simulating the pressurizer behaviour within this range of pressure with a present complex model coupled with a conventional iterative method of solving the equation of state is tremendously difficult. This is especially true when the local mechanical non-equilibrium calculation is included. A rate form of equation of state [10] is therefore implemented in the IDRIFF code, which significantly increases the stability and the efficiency of the numerical calculation [10].

The average pressure in the steam control volume P_{SA} is determined from the steam control volume specific enthalpy h_s (defined as H_s/M_s) and the average density ρ_s (defined as M_s/V_s). The rate form of equation of state for this relationship is

$$\frac{\partial P_{SA}}{\partial t} = G_1(P_{SA}, x_S)\frac{\partial h_S}{\partial t} + G_2(P_{SA}, x_S)\frac{\partial \rho_S}{\partial t} \tag{13}$$

Similarly in the liquid control volume, the average pressure P_{LA} is calculated as:

$$\frac{\partial P_{LA}}{\partial t} = G_1(P_{LA}, x_L)\frac{\partial h_L}{\partial t} + G_2(P_{LA}, x_L)\frac{\partial \rho_L}{\partial t}. \tag{14}$$

The coefficient functions G_1 and G_2 are defined as:

$$G_1(P,x) = \frac{v_g - v_f}{\left[x\frac{dh_g}{dP} + (1-x)\frac{dh_f}{dP}\right](v_g - v_f) - \left[x\frac{dv_g}{dP} + (1-x)\frac{dv_f}{dP}\right](h_g - h_f)} \tag{15}$$

and

$$G_2(P,x) = \frac{(h_g - h_f)/\rho^2}{\left[x\frac{dh_g}{dP} + (1-x)\frac{dh_f}{dP}\right](v_g - v_f) - \left[x\frac{dv_g}{dP} + (1-x)\frac{dv_f}{dP}\right](h_g - h_f)}. \tag{16}$$

Since the local mixture pressure $<P_m>$ in the drift-flux calculation is assumed to be the local saturation pressure at the grid-point, hence the equation of state for $<P_m>$ can be written similar to eqn. (13):

$$\frac{\partial <P_m>}{\partial t} = G_1(P_m, x_m) \frac{\partial \bar{h}_m}{\partial t} + G_2(P_m, x_m) \frac{\partial <\rho_m>}{\partial t}, \tag{17}$$

except that G_L and G_2 are calculated for each grid-point and are functions of local mixture pressure P_m and local mixture quality x_m.

Under the local mechanical non-equilibrium assumption, another approximated equation of state for the dispersed phase is added:

$$\frac{\partial P_d}{\partial t} = G_1(P_m, x_m) \frac{\partial \bar{h}_m}{\partial t} + G_2(P_m, x_m) \frac{\partial <\rho_m>}{\partial t} - \Delta P \frac{\partial <\alpha_d>}{\partial t} \tag{18}$$

Numerical Algorithm For Solving the Drift Flux Equations

From the four drift-flux governing equations, four main-parameters are identified as shown in Table 1.

TABLE 1. List of main-parameters

Governing equations	Main parameters
mixture continuity equation, Eqn. (7)	$<\rho_m>$
dispersed phase continuity equation, Eqn. (8)	$<\alpha_d> \rho_d$
mixture momentum equation, Eqn. (9)	$<\rho_m> v_m$
mixture energy equation, Eqn. (10)	$<\rho_m> \bar{h}_m - <P_m>$

Using a modified Crank-Nicolson semi-implicit finite difference scheme, each of the governing equations is written as a tridiagonal matrix system, with the main-parameters of all grid-points as the unknown vector.

For example, the Crank-Nicolson semi-implicit form of the mixture continuity equation (Eqn. (7)) is written as:

$$\frac{<\rho_m>_{i,j} - <\rho_m>_{i,j-1}}{\Delta t} + \frac{[(<\rho_m>_{i+1,j})(\bar{v}_{mi+1,j-1}) - (<\rho_m>_{i-1,j})(\bar{v}_{mi-1,j-1-1})]}{4\,\Delta z}$$

$$+ \frac{[(<\rho_m>_{i+1,j-1})(\bar{v}_{mi+1,j-1}) - (<\rho_m>_{i-1,j-1})(\bar{v}_{mi-1,j-1})]}{4\,\Delta z} = 0 \tag{19}$$

Hence, only the main-parameter from the equation retains its semi-implicit expression, the other are written in explicit forms.

This scheme is suitable for simulating flow condition where the change in the mixture velocity is very small, such as in the case of pressurizer. Equation (19) can further be written as:

$$-\left(\frac{\Delta t}{4\,\Delta z}\,\bar{v}_{mi-1,j-1}\right)<\rho_m>_{i-1,j}+<\rho_m>_{i,j}+\left(\frac{\Delta t}{4\,\Delta z}\,\bar{v}_{mi+1,j-1}\right)<\rho_m>_{i+1,j}$$

$$=<\rho_m>_{i,j-1}-\frac{\Delta t}{4\,\Delta z}[(<\rho_m>_{i+1,j-1})(\bar{v}_{mi+1,j-1})-(<\rho_m>_{i-1,j-1})(\bar{v}_{mi-1,j-1})]. \qquad (20)$$

or in a matrix form:

$$\bar{\bar{A}}\,\bar{U}=\bar{B} \qquad (21)$$

The matrix A is a tridiagonal matrix and U is a vector with values of the main parameters at each grid-point as its elements. This tridiagonal matrix system can be solved directly using a simple algorithm [11]. The result is the values of the main parameter at each grid-point.

Finally, knowing the values of the four main parameters, and by including the equations of state, Eqns. (17) and (18), a set of simultaneous algebraic equations is formed at each grid-point. Values of all drift-flux parameters are then solved directly.

4. EXPERIMENTAL VERIFICATION OF THE IDRIFF CODE

The IDRIFF code is used in the study of the pressurizer in order to: (a) intrapolate and extrapolate empirically obtained experimental data on quasi-steady-state conditions of the pressurizer; and (b) study the transient behaviour of the pressurizer in detail. In both, some empirical experiments are conducted on a down-scaled and extensively instrumented laboratory pressurizer loop. Simulations of the experimental conditions are then carried out by running the IDRIFF code using the same initial conditions and boundary conditions.

The experimental loop is schematically shown in the Figure 2. The pressurizer itself is a glass made cylindrical tank with an inside-diameter of 5.1 cm and a height of about 66 cm. Five immersion type electrical heaters are installed at the bottom of the tank. The heat generated from the heaters can be adjusted to a maximum of 1 Kw. A control valve and an adjustable relief valve on top of the tank are used to control a steam-bleed flow and hence to control the steam pressure in the pressurizer. A surge line is installed at the bottom of the tank which is connected to a aluminum tank, simulating the primary heat transport system. Three pressure transducers, three thermocouples and three capacitance void transducers are installed on the pressurizer. The capacitance transducers are used to measure void-fraction of the fluid [13]. Orifice flow meters are installed at the steam-bleed line and the surge line to measure flow. Using a data acquisition system, experimental data are sent to and processed in a PDP-11 computer.

The first set of experiments is to test the effect of boundary-conditions. By closing the surge-line valve and by controlling the heater power, liquid level and steam pressure to some constant values, the pressurizer fluid eventually reaches a quasi-steady-state, in which heat input from the heater is approximately balanced by the sum of heat loss through pressurizer tank wall and energy carried out by the steam-bleed flow. A step-function or a pulse-function perturbation is then introduced to one of the control parameters (heater power, steam-bleed flow and surge-line flow). The pressurizer reacts to the change and eventually reaches another quasi-steady-state. Meanwhile, the transient of the pressurizer is recorded. The following six transients were performed:

1. a step increase in heater power;
2. a step decrease in heater power;
3. a step increase in steam-bleed valve opening;

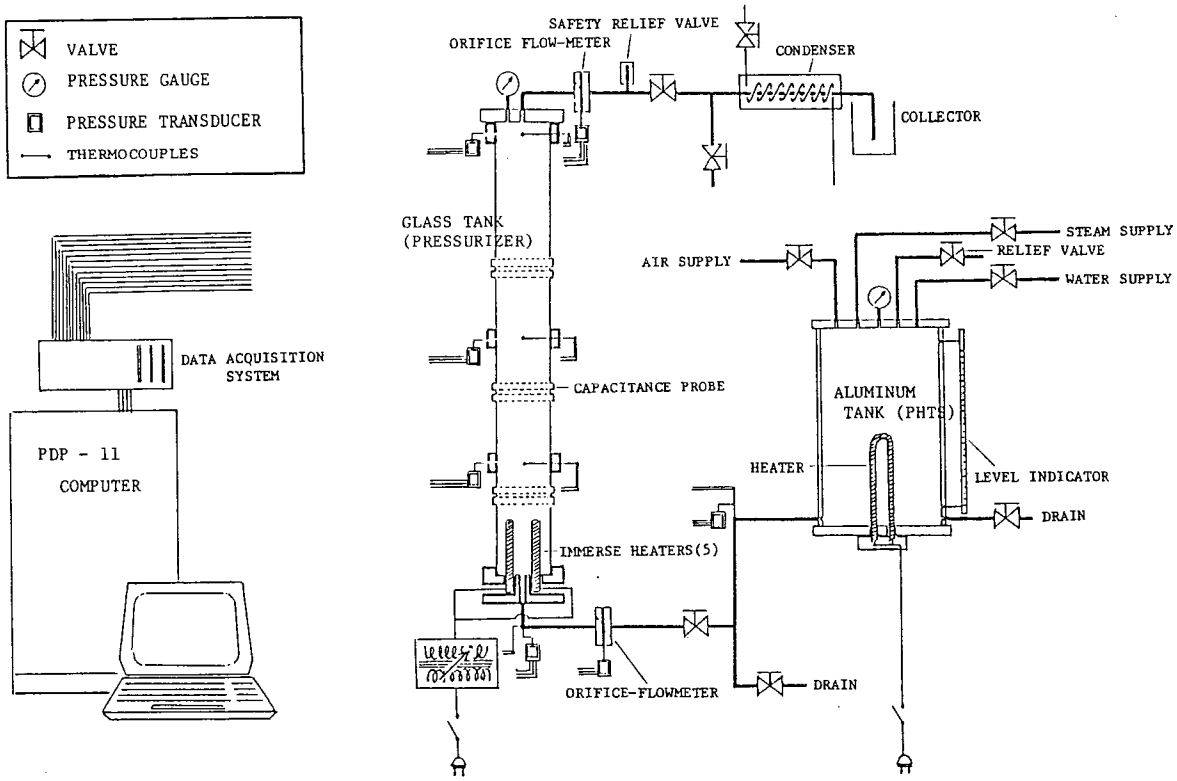

FIGURE 2. Schematic of pressurizer experimental loop.

4. a step decrease in steam-bleed valve opening;

5. a sudden and short lived outsurge from the pressurizer;

6. a sudden and short lived insurge to the pressurizer.

The purpose of these transient experiments is two-fold: First, to analyze the effect of individual parameters; second, to verify the IDRIFF code. The later will be described in the rest of this section.

Generally, the data generated from the IDRIFF simulation, which are used for comparison with experiments or for extrapolating the experimental data (Section 5), are calculated by the lumped calculations. The roles of the drift-flux calculations under these circumstances are:

(1) to generate and to verify some of the constitutive equations used in the lumped formulation which are in the forms of correlations (examples of these are the correlations for bubble rising flow in the liquid control volume and the droplet dropping flow in the steam control volume);

(2) to provide typical profiles of parameters such as pressure, temperature, phase velocity and void fraction. These are especially useful in the analysis of quasi-steady-state conditions (Section 5) where the effects of the flow-patterns on these profiles are investigated.

The simulations of the transient experiments consist of two parts: the preparation of the initial quasi-steady-state and the actual transient. Both parts are simulated by using the transient calculation of the IDRIFF code. In the first part, the values of steam pressure, liquid pressure (with correction due to any hydrostatic pressure difference), liquid temperature and liquid level of the initial 'cold' pressurizer condition measured in the experiment are input as initial conditions. Values of heaters power, ambient temperature and atmospheric pressure measured from the experiment are used as boundary conditions.

In addition, various values of the steam-bleed valve opening are tried, such that the predicted steam-bleed flow is approximately equal to the average of that measured in the experiment. The simulation is carried out until the corresponding quasi-steady-state is reached. The calculated condition of the pressurizer becomes the initial condition of the actual transient simulation.

The simulation of the actual transient is more straight-forward. Boundary conditions according to that measured in the experiment are imposed on the calculation. The simulation is carried out until another quasi-steady-state is reached. Specifically, the method of applying the boundary conditions depends on the types of the transients as follows:

(a) step-change in heater power: The electrical power to the heaters, Q_{PWR}, recorded in the experiment is inputted. The heater submodel in the code calculates values of the transient of heat input to the fluid, Q_{HEATR}, which in turn becomes the boundary condition to the numerical calculation. Steam-bleed valve opening, surge-line flow (zero flow) and other environmental conditions are maintained at their initial condition values;

(b) step-change in the steam-bleed valve opening: The steam-bleed valve opening used for the boundary condition to the calculation is varied so that the calculated steam-bleed flow changes at approximately the same rate and peaks at approximately the same values as those measured in the experiment. Heater power, surge-line flow (zero flow) and other environmental conditions are maintained at their initial condition values;

(c) perturbation of the surge flow: the experimentally measured surge flow and temperature of the fluid in the surge line (in case of insurge) are directly used as boundary conditions. Values of steam-bleed valve opening, heater power and other environmental conditions are maintained at their initial condition values.

Generally, the prediction of IDRIFF for the transient behaviour of the pressurizer is qualitatively in good agreement with that of the experiment. Moreover, the quantitative agreement on the quasi-steady-state values of all parameters, except the void fraction, are excellent. Two typical simulation results, one for step-increase in heater power (case 1) and the other for step-increase in steam-bleed valve opening (case 2) are reported in the following.

Figure 3 shows the transient of Q_{PWR}, imposed as the boundary condition, as well as the calculated transient of the Q_{HEATR} for the case 1 simulation. Figure 4 shows the calculated steam-bleed flow as a result of the imposed change in the steam-bleed valve opening in case 2. Also shown is the experimental measured steam-bleed flow for the corresponding case, which indicates a discrepancy between the two, especially after the peak. Collection of the condensed steam relieved from the steam-bleed valve in the experiment confirmed that the calculated steam-bleed flow was more realistic than the measured one. This was probably because of the presence of condensate droplets inside the valve which reduce the accuracy of the steam flow measurement.

The comparison of the transients predicted by the IDRIFF code and that measured in the experiment for the case 1 are shown in Figs. 5a to 5f. In Figs. 5a and 5b, the increase in the discrepancy between predicted pressures and measured pressures after about 200 seconds is probably due to the fact that only one type of heat transfer coefficient is used in the heater submodel. However, the values of those predicted and those measured at both the initial and final quasi-steady-states agrees extremely well. In Fig. 5b, the liquid pressure predicted by the IDRIFF code is an average value over the whole liquid control volume while the one in the experiment is measured at a location slightly lower than the centre of the height of the liquid level. This explains the greater discrepancy of the liquid pressure in Fig. 5b than that of the steam pressure in Fig. 5a. The transients of the temperatures in Figs. 5c and 5d basically follow the same tendencies of that of pressure. In Fig. 5e, it is noted that the value of the void fraction in the liquid control volume predicted by the IDRIFF code and that measured in the experiment differs by about 20% (or 0.09 in absolute value) at the initial quasi-steady-state, which is within the maximum experimental error of capacitance method of void fraction measurement. The sudden increase in the

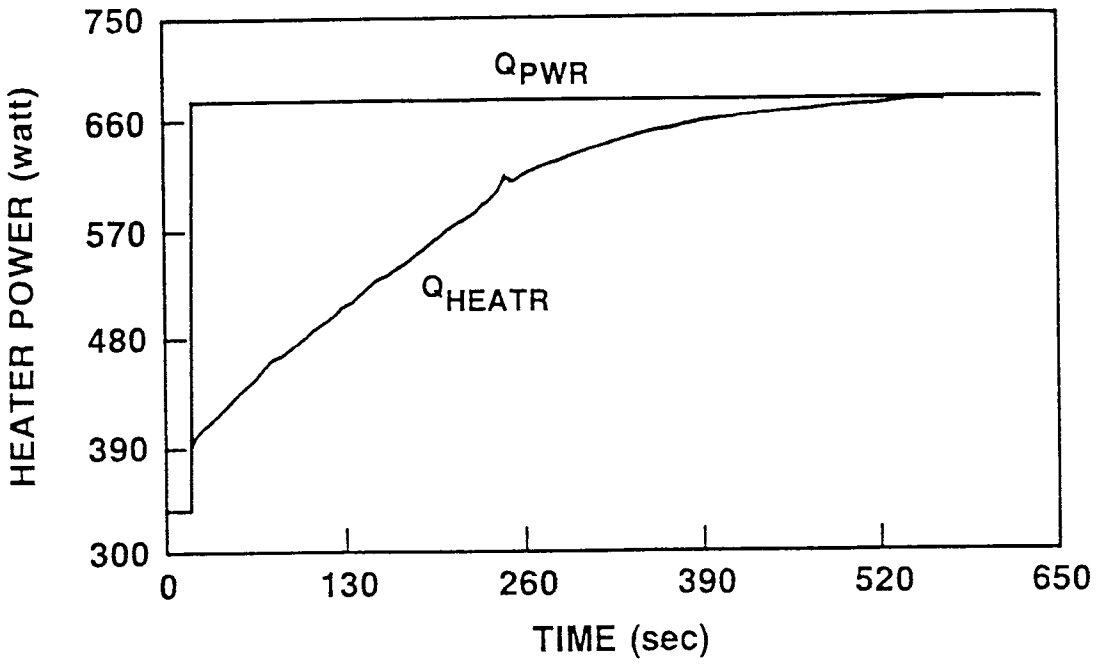

FIGURE 3. Case 1: step increase in heater electrical power and actual power transient to liquid.

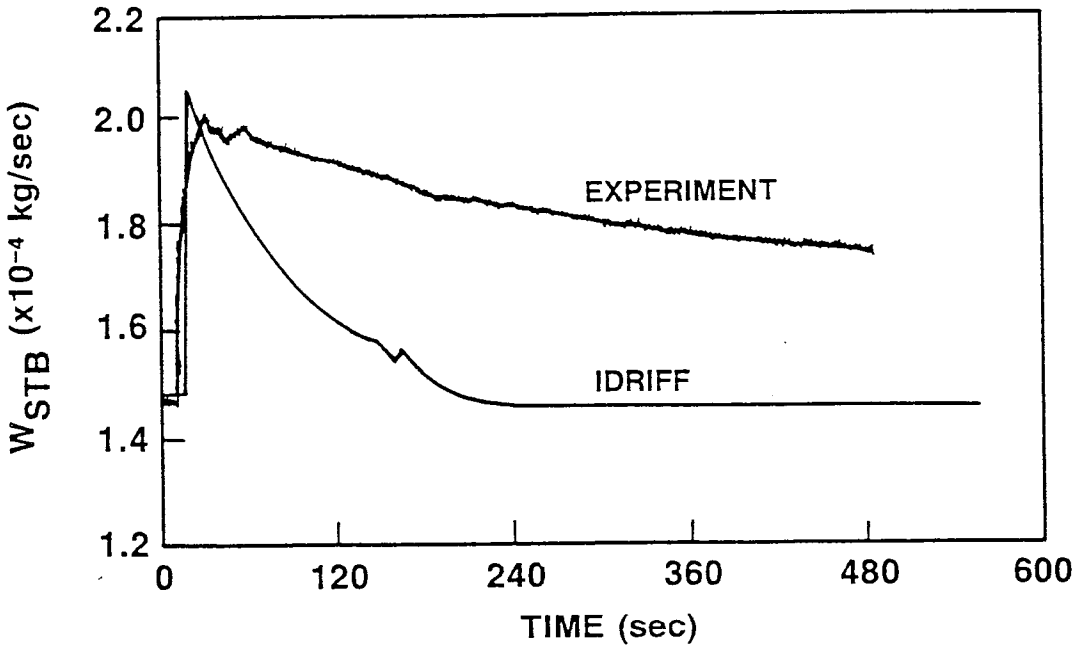

FIGURE 4. Case 2: transient of steam-bleed flow due to step increase in steam-bleed valve opening.

discrepancy between the predicted void fraction and the measured void fraction after about 400 seconds is probably due to the transitions of flow-regimes in the pressurizer, which may reduce the accuracy of the void fraction measurement, as well as requires changes in the constitutive equations in the IDRIFF code. Finally, in Fig. 5f, the experimental values of the liquid level are measured from photographs taken. The discrepancies between that predicted and that measured are within experimental error.

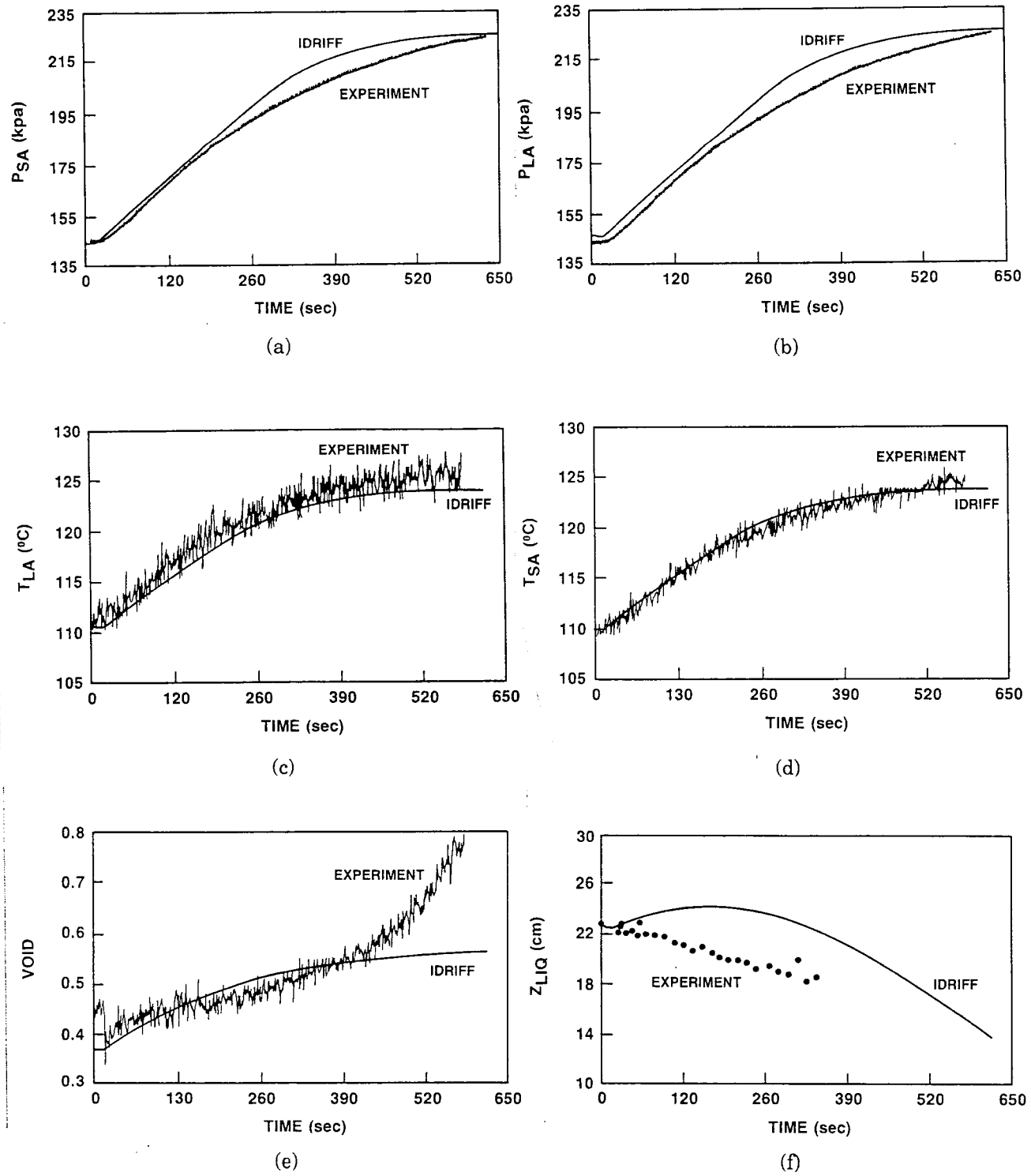

FIGURE 5. Case 1: Transients of pressures and temperatures in steam volume and liquid volume, void fraction in liquid volume and liquid level.

Figures 6a and 6b show the comparison between the predicted and experimentally measured pressures in the steam and liquid control volumes, respectively. The temperature comparison are shown in Figs. 6c and 6d. The void fractions in the liquid control volume are compared in Fig. 6e and the liquid levels in Fig. 6f.

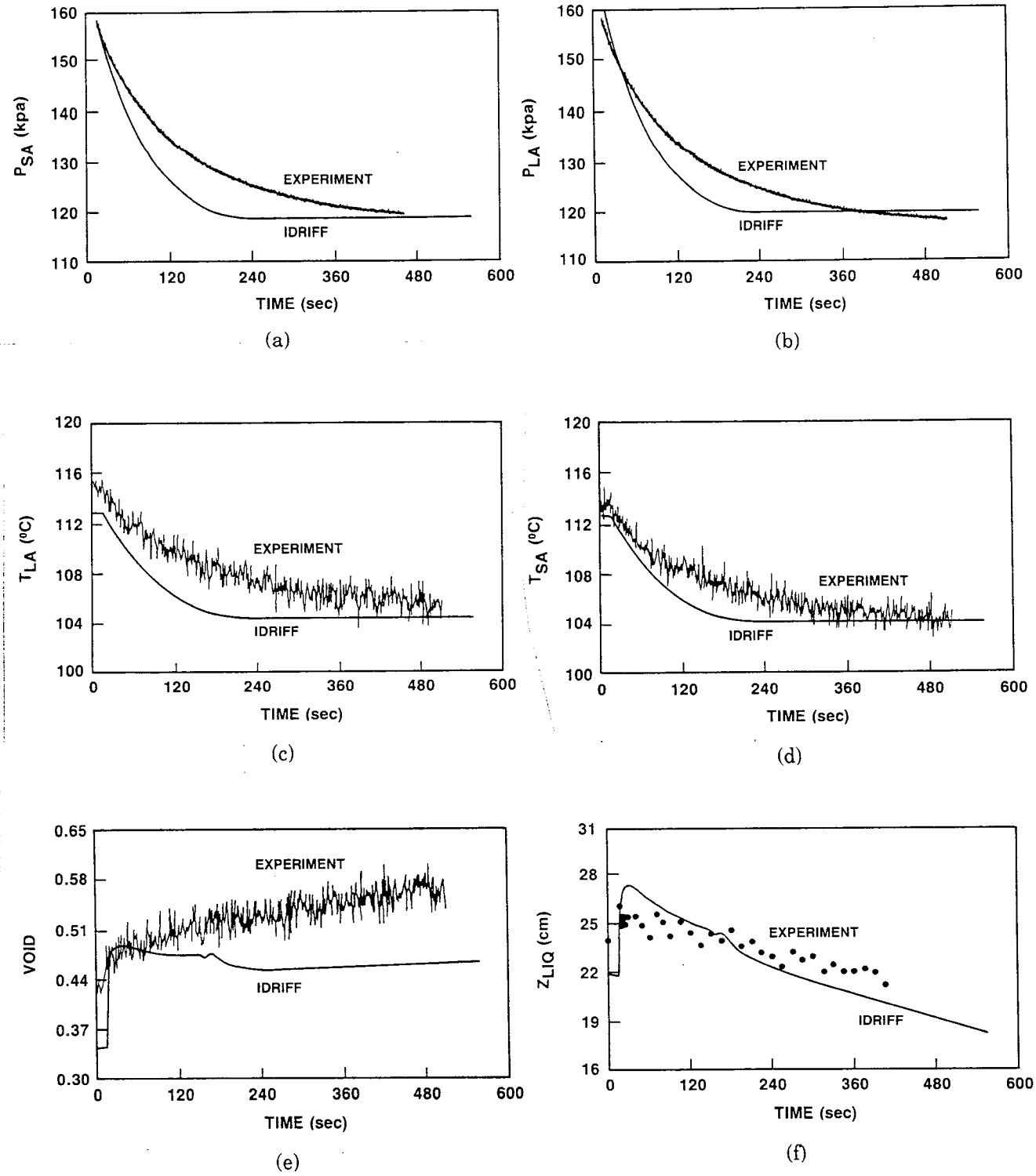

FIGURE 6. Case 2: Transients of pressure and temperatures in steam volume and liquid volume, void fraction in liquid volume and liquid level.

The differences between the slopes of the predicted and measured pressures and temperature transients, from time = 0 sec. to about 400 secs., indicate that the predicted pressures and temperatures decrease at different rates than those measured. The greatest contributing factor to the discrepancy may be the characteristic of the steam-bleed valve. Due to the condensation of steam and the presence of droplets at or near the steam-bleed valve in the experiment, the nature of the actual steam-bleed valve character-

istic is much more complex than that ideally modelled in the IDRIFF code. The increasing discrepancy in the void fraction is, again, probably due to the transition of flow pattern, and hence, inaccuracy of measurement in the experiment and/or incorrect use of constitutive equation in the simulation.

5. THE QUASI-STEADY-STATE EXPERIMENT

Systematic study of the phenomena in the pressurizer for the quasi-steady-state is an important aspect of the pressure study. Among the things to be investigated are pressurizer flow patterns and their transitions, and relationships among the various parameters under quasi-steady-states.

The quasi-steady-state experiments include combinations of heater power, steam relief valve set-points and liquid levels. In all, 78 sets of quasi-steady-states experiments wre performed. In each of them, the flow patterns within both the liquid control volume and the steam control volume are visually observed; the swelled liquid level is measured; the pressure, temperature and void fraction of the fluid, the steam-bleed flow and heater power wre recorded.

It was determined that the flow-pattern of the fluid depends on pressurizer pressure, liquid level and heater power. These are summarized as a "raw" form of flow-regime map as shown in Fig. 7. The effect of the pressure is discretely represented by three sets of lines, each ranging from 60 kpa(a) to 200 kpa(a). For each pressure, three different lines (one solid line, one dashed line and one broken line) of the corresponding pressure separate the area on the map into four different regimes. These regimes represent four different flow-patterns in the liquid control volume and two different flow-patterns in the steam control volume which will occur at that particular pressure.

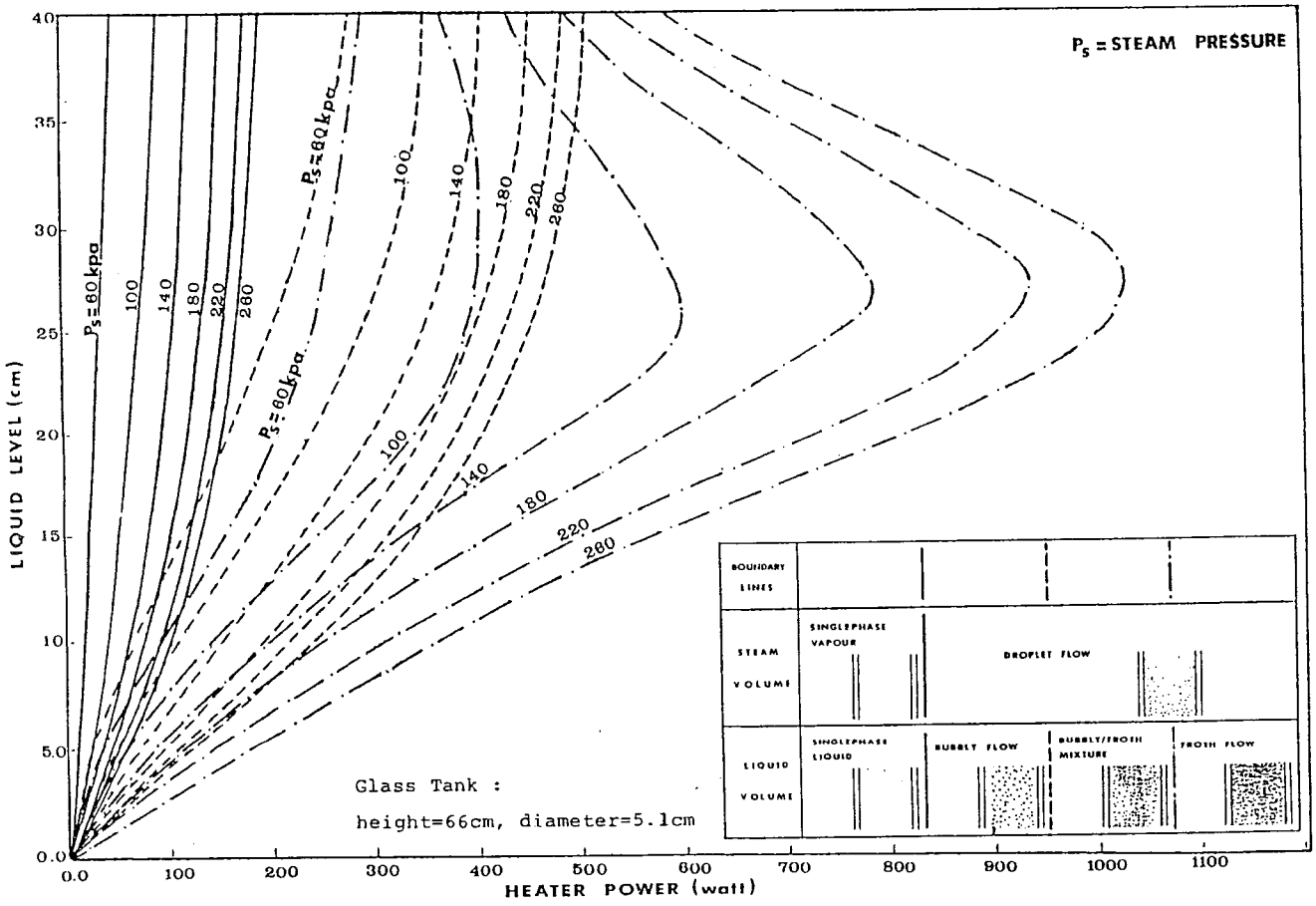

FIGURE 7. Pressurizer flow-pattern as a function of liquid level, heater power and steam pressure.

The pressure, temperature and void fraction are measured at a finite number of locations. The axial profiles of these parameters and values of other parameters such as bubble velocity, heat loss to the wall, etc., are simply not available. By using the IDRIFF code to simulate the same quasi-steady-state experiment, the availability of information, such as profiles of parameters and interfacial mass and energy transfer, is significantly increased. In addition, the consistency, if not the accuracy, of the already existing experimental parameters' values is greatly improved. The following examples of considerations elaborate this aspect.

1. Steam-bleed flow rate. In the experiment, the steam-bleed flow orifice flow meter is calibrated using dry steam. However, during the experiment, carry-over of liquid into the orifice flow meter sometimes occurs, and the accuracy and the consistency of the flow rate measurements is highly distorted. On the other hand, the accuracy of numerical calculation of the steam-bleed flow depends on the modelling of the relief valve, which is of course consistent. Verification of the model is done by comparing the numerically predicted value and the actual measured value of the flow in the experimental runs where no carry-over of liquid is observed;

2. Void fraction measurement. The accuracy of the capacitance method of void fraction measurement was found to be about 0.08 (absolute value) in error. Any effect of a smaller change in the void fraction on the condition in the pressurizer may be overlooked if a more accurate and independent calculation of the void fraction is not used;

3. The averaged liquid level at liquid swelling condition. The measurement of liquid level during the experiment is occasionally very difficult due to the violent movement of the steam-liquid interface. However, using the initial liquid level, hence the initial fluid inventory, as an initial condition to the numerical simulation, and using the liquid level after the cool-down condition for verification, consistent numerical determination of the averaged liquid level during a quasi-steady-state condition can be obtained.

The procedure for simulation of the quasi-steady-state experiment is basically like that for setting-up the initial quasi-steady-state condition in the transient simulation. The only exception is that there is no experimenting with the steam-bleed valve opening. Instead, a fixed steam relief valve set point is used as a boundary condition. The transient calculation of the simulation uses constant boundary conditions. The simulation is carried out until the final quasi-steady-state is as similar as possible to the actual quasi-steady-state in the experiment. The similarity is verified by comparing the values of steam pressure, liquid temperature, heater power (exact), relief valve set-point (exact), local phase velocity profiles (to indicate different flow pattern) and the liquid level. The inventories of fluid at the initial and final "cold" conditions are also used to verify the total mass inventory in the numerical calculation. The maximum discrepancies between the predicted values and the measured values of major parameters are listed in Table 2.

It is noted that attempts were made to impose experimentally measured void fraction in the liquid volume as an initial condition to the simulation. However, the numerical simulation seems to favour its own unique value for each different set of quasi-steady-state condition. This is because the void fraction is a property of the system which depends on the thermodynamic condition of the pressurizer. The latter is, in turn, controlled by the boundary conditions. The calculated value, instead of the experimentally measured value of the void fraction, is therefore chosen as the representative one in the analysis since it is more consistent with the mass and energy content of the pressurizer. As shown in Table 2, the discrepancy between the numerically predicted void fraction and the experimentally measured one can be as high as 29%, in some cases, although it is always less than void fraction experimental error.

A complete and systematically organized data set on the pressurizer quasi-steady-state has been set up based on both the empirical experiment and the numerical extrapolation. Initial analysis of the data has produced several useful results[14]. Some of them will be briefly described in the following.

The first result is the finding of relationships between the void fraction in the liquid volume and pressurizer boundary conditions. Defining two dimensionless parameters Q^* and W^* as:

TABLE 2. Maximum discrepancies between values of parameters predicted by IDRIFF code and that measured in experiment at quasi-steady-state.

PARAMETERS	MAX. DISCREPANCY (%)
steam pressure	0.2
liquid pressure	1.0
steam temperature	0.5
liquid temperature	1.0
steam (dry)–bleed flow	1.7
swelled liquid level	3.0
void fraction in liquid volume	29.0

$$Q^* = \frac{4}{\pi D^2} \frac{(Q_{PWR} - Q_{WL} - Q_{WS})(\rho_f - \rho_g)^{3/4}}{(h_g - h_f)\rho_f^{1/2}\rho_g(g\sigma)^{1/4}}$$

$$W^* = \frac{4}{\pi D^2} \frac{W_{STB}\rho_f^{1/2}}{\rho_g[g\sigma(\rho_f - \rho_g)]^{1/4}}$$

where Q_{PWR} is heater power, Q_{WL} and Q_{WS} are heat loss through pressurizer wall, W_{STB} is the steam-bleed flow. Q^* and W^* are some kinds of Kutadeledse number. Figures 8 and 9 show the dependencies of the void fraction in the liquid volume on Q^* and W^*. Also shown are lines representing some suggested semi-analytical correlations. These relationships are very useful in the operation of actual pressurizer, where the void fraction inside the pressurizer metal vessel can now be estimated as a function of the measurable boundary conditions.

Another result is the development of a generalized pressurizer flow regime map. Figure 10 shows the final form of the map converted, with the help of simulation by IDRIFF, from the 'raw' form in Fig. 7. Through analysis, the effects of the three parameters in Fig. 7 can be shown to be represented by the two coordinates in Fig. 10, which are the void fraction in liquid volume and a dimensionless liquid level $L^*(= z_{LIQ}/D)$.

6. CONCLUSION

The IDRIFF two-phase simulation code has been briefly described. The dual component nature of its modelling enables the code to become highly flexible and useful in a wide range of two-phase flow applications. The technique of applying the IDRIFF code to simulate both the transient and quasi-steady-state of a laboratory pressurizer has also been discussed. The following can be concluded:

1. The IDRIFF code predicts the transient behaviour of all the pressurizer parameters with reasonably good agreement qualitatively. Moreover, quantitative discrepancies between values of pressure and temperature calculated by IDRIFF and those experimentally measured are within 8% during the transient. The discrepancy for the liquid level varies between zero to 20%.

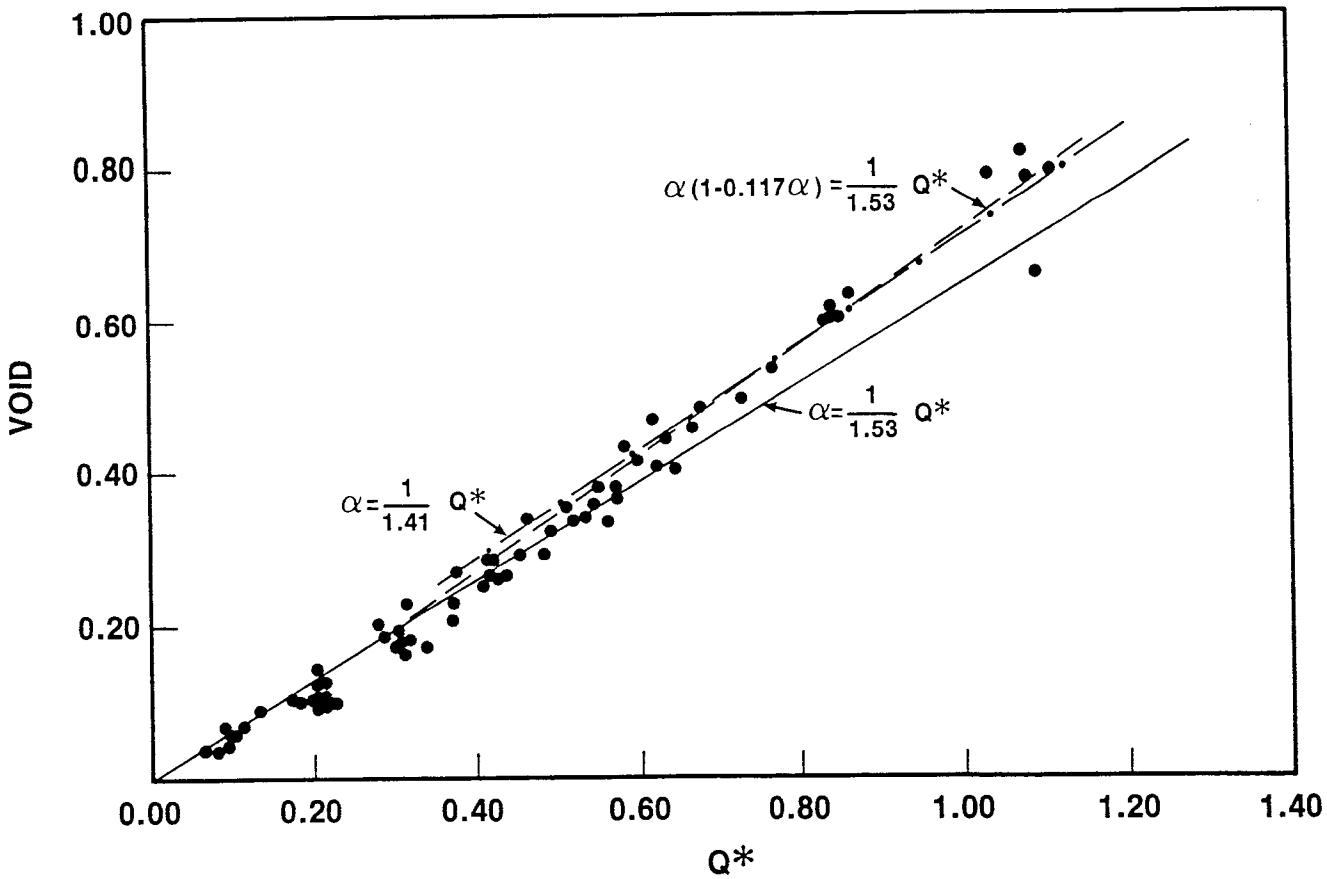

FIGURE 8. Void fraction in liquid volume as a function of parameter Q*.

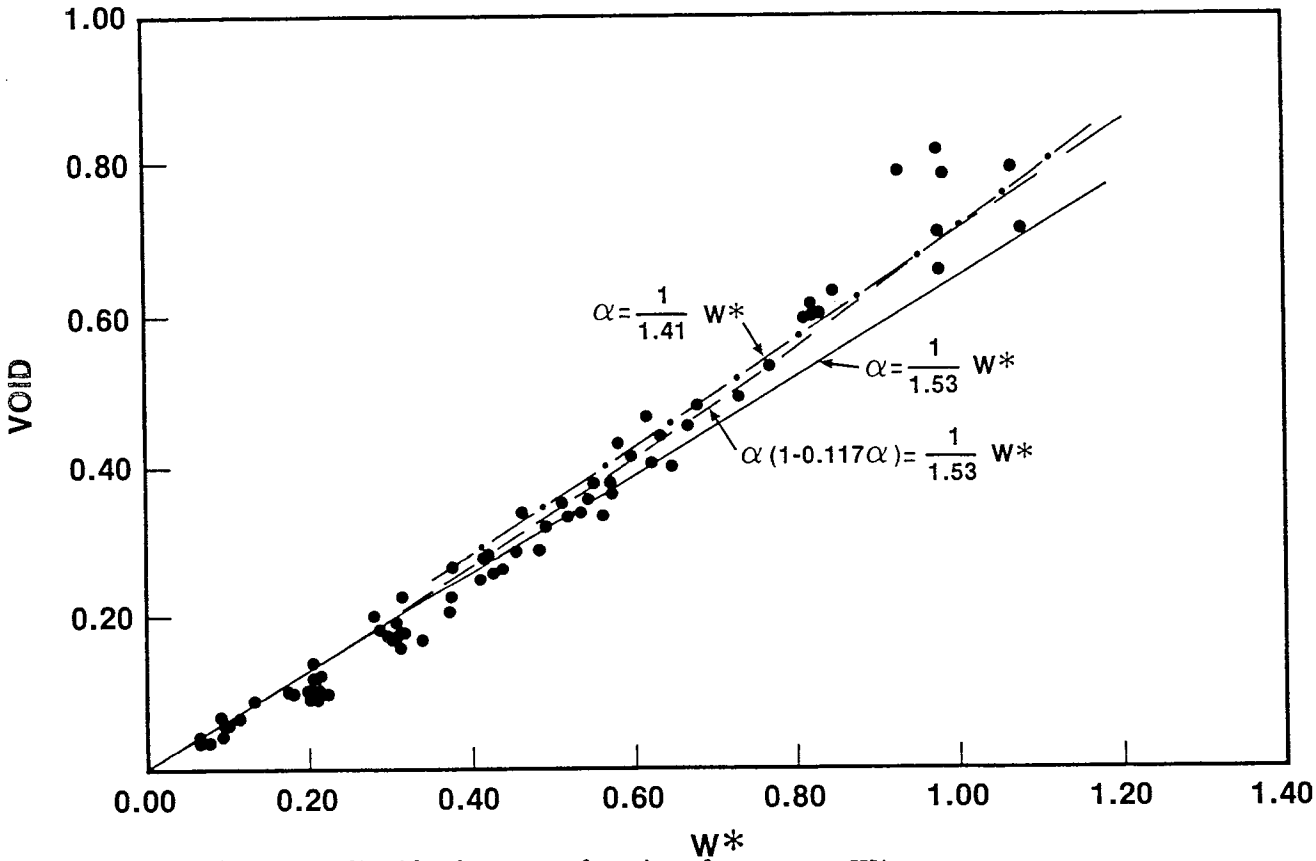

FIGURE 9. Void fraction in liquid volume as a function of parameter W*.

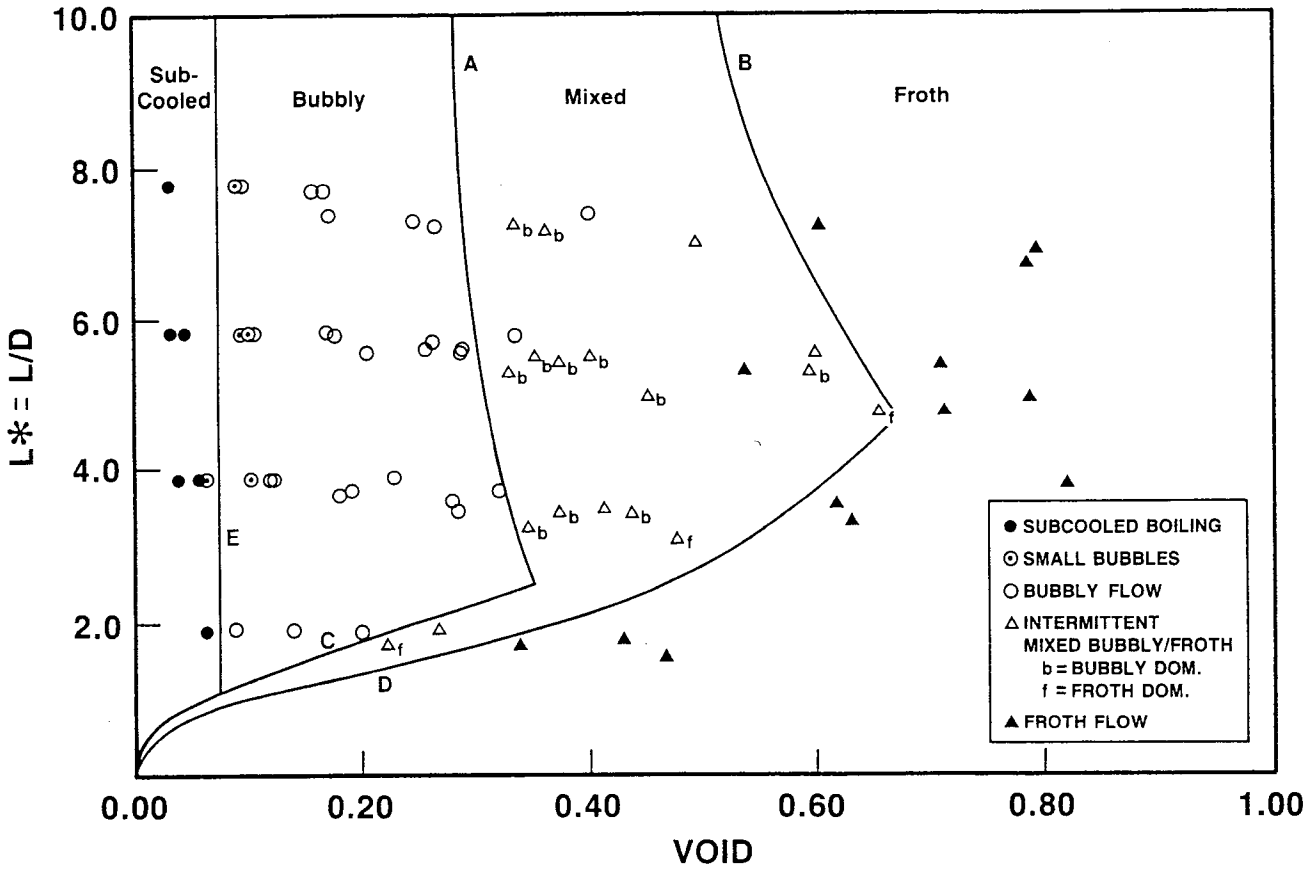

FIGURE 10. Pressurizer flow regime map.

2. The IDRIFF code predicts the values of all pressurizer parameters, except void fraction, at the quasi-steady-state condition within 3% accuracy. The discrepancy for the void fraction is less than 29%.

3. Using the IDRIFF code to intrapolate and extrapolate pressurizer quasi-steady-state experimental data significantly increases the availability of the information, as well as improves the consistency of the experimental data. The combined empirical-numerical data provide a base for the analyses of the pressurizer phenomena. Initial stages of the analysis have produced relationships between the void fraction in the liquid volume and pressurizer boundary conditions, and a flow regime map of the pressurizer under quasi-steady-state conditions.

NOMENCLATURE[1]

A	Pressurizer cross-sectional area
D	Pressurizer cross-sectional diameter
f_m	Two-phase flow friction coefficient (D)
G_1, G_2	Coefficient functions in the rate form of equation of state
g	Acceleration due to gravity

1 The letters 'L' or 'D' within parentheses at the end of some definition indicates whether the parameter defined is specifically used in the Lumped calculation or in the Drift-flux calculation.

g_z	Component of the gravitational acceleration in the axial direction (D)
h_f	Saturated liquid phase specific enthalpy
h_{fLQ}	Average saturated liquid phase specific enthalpy in the liquid control volume (L)
h_{fST}	Average saturated liquid phase specific enthalpy in the steam control volume (L)
h_g	Saturated gas phase specific enthalpy
h_{gLQ}	Average saturated gas phase specific enthalpy in the liquid control volume (L)
h_{gST}	Average saturated gas phase specific enthalpy in the steam control volume (L)
h_S	Average specific enthalpy of mixture in the steam control volume (L)
h_L	Average specific enthalpy of mixture in the liquid control volume (L)
h_c	Local continum phase specific enthalpy (D)
h_d	Local dispersed phase specific enthalpy (D)
h_m	Local mixture specific enthalpy (D)
h_{SRL}	Specific enthalpy of the fluid in the surge line (L)
M_L	Total mass of mixture in the liquid control volume (L)
M_m	Local interfacial momentum source (D)
M_S	Total mass of mixture in the steam control volume (L)
P	Pressure
P_{LA}	Average pressure in the liquid control volume (L)
P_m	Local mixture pressure (D)
P_{SA}	Average pressure in the steam control volume (L)
Q_{COND}	Rate of energy released by the condensing steam at the interface (L)
Q_{EVPR}	Rate of energy absorbed by the evaporating liquid at the interface (L)
Q_{HEATR}	Actual heat input to the pressurizer fluid from the heaters (L)
Q_{PWR}	Electrical power to the heaters (L)
Q_{TR}	Heat transfer rate from the liquid control volume to the steam control volume due to the temperature gradient (L)
Q_{WL}	Heat loss to the environment through portion of pressurizer wall surrounding the liquid control volume (L)
Q_{WS}	Heat loss to the environment through portion of pressurizer wall surrounding the steam control volume (L)
q	Local conduction heat flux (D)
q^T	Local turbulent diffusion flux of energy (D)
q_w''	Local wall heat flux (D)
t	Time
T_{LA}	Average temperature in the liquid control volume (L)
T_{SA}	Average temperature in the steam control volume (L)
V_L	Volume of mixture in the liquid control volume (l)
VOID	Average void fraction in the liquid control volume (L)
V_S	Volume of the mixture in the steam control volume (L)

v_c	Local continum phase velocity (D)
v_d	Local dispersed phase velocity (D)
v_{dj}	Drift velocity (D)
v_f	Saturated liquid phase specific volume
v_g	Saturated gas phase specific volume
v_m	Local mixture velocity (D)
W_{BR}	Flow of bubbles from the bulk of the liquid control volume rising toward the steam control volume (L)
W_{CD}	Flow of condensate droplets from the bulk of the steam control volume toward the liquid volume (L)
W_{CI}	Interface condensation rate (L)
W_{EI}	Interface evaporation rate (L)
W_{SRL}	Surge-line flow (L)
W_{STB}	Steam-bleed flow (L)
x	Steam quality
x_L	Average steam quality in the liquid control volume (L)
x_m	Local mixture steam quality (D)
x_S	Average steam quality in the steam control volume (L)
z	Axial distance (D)
z_{LIQ}	Height of the liquid control volume (L)

Greek Symbols

α_c	Local continum phase volume fraction (D)
α_d	Local dispersed phase volume fraction (D)
β	Portion of energy exchange during interface evaporation or condensation that is absorbed or released by the liquid control (L)
Δ_{hdc}	Difference between specific enthalpy of the two phases (D)
ΔP	Local inter-phase pressure difference (D)
δ	Portion of Q_{COND} that is lost to the wall (L)
Γ_d	Rate of local interfacial mass transfer for the dispersed phase due to phase change (D)
$\Phi_m{}^{\mu}$	Local mixture viscous dissipation term (D)
$\Phi_m{}^{\sigma}$	Work due to surface tension force (D)
$\Phi_m{}^{i}$	Local interfacial mechanical energy transfer term (D)
ρ_c	Local continuum phase density (D)
ρ_d	Local dispersed phase density (D)
ρ_L	Average density of mixture in the liquid control volume (L)
ρ_m	Local mixture density (D)
ρ_f	Saturated liquid phase density
ρ_g	Saturated gas phase density

ρ_S Average density of mixture in the steam control volume (L)

τ_{zz} Normal component of mixture viscous stress (D)

τ_{zz}^T Normal component of mixture turbulent stress (D)

ξ_h Heated parameter (D)

Operation Symbols:

area average:

$$<F> = \frac{1}{A} \int_A F \, dA$$

phase volume-fraction weight mean value:

$$<<F_k>> = \frac{<\alpha_k F_k>}{<\alpha_k>}$$

mixture average parameter:

$$\bar{\Psi}_m = \frac{[<\alpha_d> \rho_d <<\Psi_d>> + (1 - <\alpha_d>) \rho_c <<\Psi_c>>]}{<\rho_m>}, \qquad \Psi = h, v$$

covariance term:

$$COV(\alpha_k \rho_k \Psi_k v_k) = <\alpha_k \rho_k \Psi_k (v_k - <<v_k>>)>, \qquad \Psi = h, v$$

REFERENCES

1. D.J. Gorman, "Steam Surge Tank Transient During Outsurge", ASME Paper No. 9-WA/NE-14, 1969.

2. A.N. Nahavandi and S. Makkenchery, "An Improved Pressurizer Model with Bubble Rise and Condensate Drop Dynamics", Nuc. Eng. & Design, Vol. 12, p. 135, 1970.

3. B. Baggoura and W. Martin, "Transient Analysis of the Three Mile Island Unit 2 Pressurizer System", Nuclear Technology, vol. 62, p. 159 1983.

4. S.M. Sami, "A Dynamic Model for Predicting CANDU Pressurizers Performance", Nuclear Technology, vol. 72, p. 7, 1986.

5. S.N. Kim and P. Griffith, "PWR Pressurizers Modelling", Proc. of Specialists Meeting on Small Break LOCA Analysis in LWR's, p. 207, 1985.

6. J.C.Lin, R.A. Riembe, V.H. Ransom and G.W. Johnson, "RELAPS/Mode Pressurizer Modelling", ASME paper No. 84-WA/HT-86.

7. W. Wulff, H.S. Cheng, A.N. Mallen and A. Stritar, "Kinematics of Two-Phase Mixture Level Motion in BWR Pressure Vessels", Proc. of Specialists Meeting on Small Break LOCA Analysis in LWR's, p. 193, 1985.

8. R. Sollychin, W.J. Garland and J.S. Chang. "Development and Applications of IDRIFF Two-Phase Simulation Code", CNS 12th Symp. Simul. Reac. Dymc. Plant. Contr., Hamilton, Canada, April 1986, Paper No. 2A-1.

9. M. Ishii, "Thermo-fluid Dynamic Theory of Two-Phase", Chapters IX and X, Eyrolles, Paris, France (1975).

10. W.J. Garland and R. Sollychin. "The Rate Form of the Equation of State for Thermodynamic Systems", CNS/ANS 2nd Int. Conf. Num. Meth. Nuc. Eng., Montreal, Canada, Oct. 1986.

11. D. Greenspan, "Discrete Numerical Methods for Physics and Engineering", Chapter 1, Academic Press Inc. (1974).

12. P. De Melker and D.O.H. Latzko, "Digital Analysis of Pressurizer Transients and Comparison with Experimental REsults", Symp. in Two-Phase Flow Dynamics, Eindhoven, p. 1397, 1969.

13. J.S. Chang, R. Girald, R. Raman and F.B.P. Tran, "Measurement of Void Fraction In Vertical Gas-Liquid Two-Phase Flow By Ring Type Capacitance Transducers", A.S.M.E. Press, New York, 1974.

14. R. Sollychin, W.J. Garland and J.S. Chang, "Two-Phase Flow Patterns and Their Transitions in Pressurizers Under Quasi-Steady-State", (to be published).